Novel functionalized pyridine-containing DTPA-like ligand. Synthesis, computational studies and characterization of the corresponding Gd^{III} complex†

Roberto Artali,[a] Mauro Botta,*[b] Camilla Cavallotti,[c] Giovanni B. Giovenzana,[d] Giovanni Palmisano[e] and Massimo Sisti*[e]

Received 24th April 2007, Accepted 4th June 2007
First published as an Advance Article on the web 25th June 2007
DOI: 10.1039/b706236b

A novel pyridine-containing DTPA-like ligand, carrying additional hydroxymethyl groups on the pyridine side-arms, was synthesized in 5 steps. The corresponding Gd^{III} complex, potentially useful as an MRI contrast agent, was prepared and characterized in detail by relaxometric methods and its structure modeled by computational methods.

Introduction

Complexes of trivalent lanthanide cations are currently employed in several areas of chemistry, material science, biology and medicine.[1] The large and increasing interest for these compounds is explained by the rich variety of magnetic, optical and radiochemical properties associated with the different metal ions of the lanthanide series that can be partly modulated by controlling the stereochemical and electronic properties of their complexes. At the same time, the chemical and structural properties of the lanthanide complexes typically show only minor variations across the series as a function of the atomic number, thus simplifying their characterization. In fact, information gained on a complex of a given Ln^{III} cation can often be safely assumed to apply to a different metal ion.

A further, great impulse to the study of these compounds has been given by the advent of magnetic resonance imaging (MRI)[2,3] into clinical practice as a fundamental diagnostic technique and the concomitant discovery that Gd^{III} chelates could markedly improve the image contrast and thus their diagnostic information content. Finally, in recent years we have observed a growing importance of various radionuclides for use in both molecular imaging and therapy; even in nuclear medicine, lanthanides ions play a significant role.[4]

For biomedical *in vivo* applications toxicity is a major concern and then the Ln^{III} cation needs to be strongly complexed in order to avoid dissociation under physiological conditions. As the trivalent lanthanide ions typically exhibit a coordination number (CN) of 8–10, this requirement implies the use of chelators with a denticity of 6–8 in order to obtain complexes endowed with a sufficiently high thermodynamic stability. In addition, complexes with macrocyclic ligands are characterized by a marked kinetic inertness towards acid catalyzed dissociation. Polyaminocarboxylic acids represent the most common and studied class of chelators for biomedical applications. The complex $[Gd(DTPA)(H_2O)]^{2-}$ (DTPA = diethylenetriamine-*N*,*N*,*N*′,*N*″,*N*″-pentaacetic acid), commercially known as Magnevist®, was the first contrast enhancing agent (CA) to be approved for *in vivo* use in MRI.[3] The bis-methylamide derivative, GdDTPA-BMA (Omniscan®), was also introduced into clinical practice with the aim of reducing the osmotic potential in the case of applications requiring high doses of CA.

For all the different applications in biomedical studies the improvement in the properties of the probe is closely related to a better understanding of the relationship between the details of the solution structure and the physico-chemical properties of the Ln chelates. Furthermore, a rational modification of the ligand backbone with different donor groups can affect not only its coordinating ability but also the size, the charge, and the lipophilicity of the corresponding complexes thus affecting their affinity for different biological targets. The success of Ln^{III} complexes with DTPA-like ligands has stimulated further studies based on the modification of their basic structure,[3b,5–6] but, to the best of our knowledge, the substitution of structurally different chelating groups on the 1,4,7-triazaheptane skeleton has been scarcely investigated. The contribution of various donor groups to the stability of lanthanide complexes has been evaluated on different ligand platforms and some indications of their relative stability are now available.[7]

For this reason, we reasoned that the replacement of the two CH_2COOH moieties on N-1 and N-7 (1,4,7-triazaheptane numbering) by 6-hydroxymethyl-2-pyridylmethyl groups in the DTPA structure would possibly lead to a novel, potentially octadentate and efficient chelator for Ln^{III} ions (**1**, Fig. 1). The

[a]*Istituto di Chimica Farmaceutica e Tossicologica "Pietro Pratesi", Università degli Studi di Milano, Viale Abruzzi 42, 20131 Milano, Italy. E-mail: roberto.artali@tiscali.it*
[b]*Dipartimento di Scienze dell'Ambiente e della Vita, Università del Piemonte Orientale "A. Avogadro", Via Bellini 25/G, 15100 Alessandria, Italy. E-mail: mauro.botta@mfn.unipmn.it*
[c]*CAGE Chemicals, Via Quarello 11/a, 10135 Torino, Italy. E-mail: cagechemicals@yahoo.it*
[d]*Dipartimento di Scienze Chimiche Alimentari Farmaceutiche e Farmacologiche & DFB Center, Università degli Studi del Piemonte Orientale "A. Avogadro", Via Bovio 6, 28100 Novara, Italy. E-mail: giovenzana@pharm.unipmn.it; Fax: +39-0321-375821; Tel: +39-0321-375746*
[e]*Dipartimento di Scienze Chimiche e Ambientali, Università degli Studi dell'Insubria, Via Valleggio 11, 22100 Como, Italy. E-mail: massimo.sisti@uninsubria.it; Fax: +39-031-2386449; Tel: +39-031-2386440*
† Electronic supplementary information (ESI) available: pH-dependence of the relaxation rate for Gd-**1**. See DOI: 10.1039/b706236b

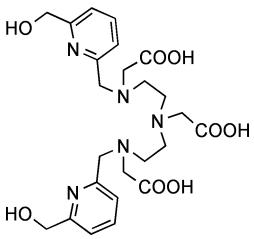

Fig. 1 Ligand **1**.

corresponding neutral complexes should be characterized by a thermodynamic stability comparable to that of the LnDTPA-BMA chelates. In addition, the hydroxymethyl moieties would provide suitable handles for further functionalizations, thereby facilitating the molecular recognition towards specific targets. Functionalization offers the possibility to modulate several properties of the complexes, *i.e.* liphophilicity, size, charge by means of an appropriate choice of the substituents at the O-atoms. Here we report on the synthesis of the ligand **1** and the characterization of its Gd complex by computational studies and ^{1}H and ^{17}O NMR relaxometric techniques.

Synthesis of ligand 1

The synthetic pathway we envisioned for the preparation of ligand **1** is depicted in Scheme 1.

The commercially available 2,6-di(hydroxymethyl)pyridine was monooxidized with manganese dioxide in chloroform under reflux (according to the procedure described by Ziessel and coworkers)[8] affording 6-hydroxymethyl-pyridine-2-carboxaldehyde **3** in 70% isolated yield. Subsequent reaction of **3** with 1,4,7-triazaheptane in dichloromethane in the presence of anhydrous sodium sulfate gave the diimine **4**. Simple evaporation of the reaction mixture allowed the quantitative recovery of **4** which could be used without further purification. Reduction of **4** with sodium borohydride in refluxing ethanol led to the isolation of the derivative **5** in 70% overall yield from **3** after purification by silica gel chromatography. Attempts were made in order to perform the reductive amination of **3** in one step. Treatment of **3** with 1,4,7-triazaheptane in the presence of sodium cyanoborohydride or triacetoxyborohydride[9] in methanol or ethanol proved troublesome, affording a complex reaction mixture where the desired compound **5** could be isolated in poor yields. The success of the alkylation step of **5** with *t*-butyl bromoacetate leading to **6** strongly depended on the solvent used. The best results were uniformly obtained with *N*-methylpyrrolidone in the presence of anhydrous potassium carbonate at 60 °C (75% yield after purification by silica gel chromatography). Conversely, the use of *N*,*N*-dimethylformamide or acetonitrile, which were successfully employed as solvents in alkylation reactions on polyamines, led to sluggish and incomplete conversion. Furthermore, treatment of **5** with oxoacetic acid in the presence of sodium cyanoborohydride[10] or triacetoxyborohydride with the aim of obtaining directly ligand **1** gave unsatisfactory results (yields <5%). Unmasking of **6** with trifluoroacetic acid followed by evaporation in vacuum and treatment with diethyl ether to induce precipitation of the ligand, gave **1** in 63% yield, pure enough for the subsequent studies. Ligand **1** was fully characterized by means of high resolution ^{1}H- and ^{13}C-NMR spectra and mass spectra.

Structure modeling

In the absence of the X-ray crystal structure, the ground state geometries were obtained by molecular mechanics methods and all the potential starting arrangements of the donor atoms around the Gd^{III} metal ion for ligand **1** were considered. The most promising results were then refined using quantum chemical semiempirical methods, giving rise to a set of low-energy structures (Table 1).

For molecular mechanics calculations, an extension of the MM2 force field for Gd^{III} complexes[11] was used. Semiempirical

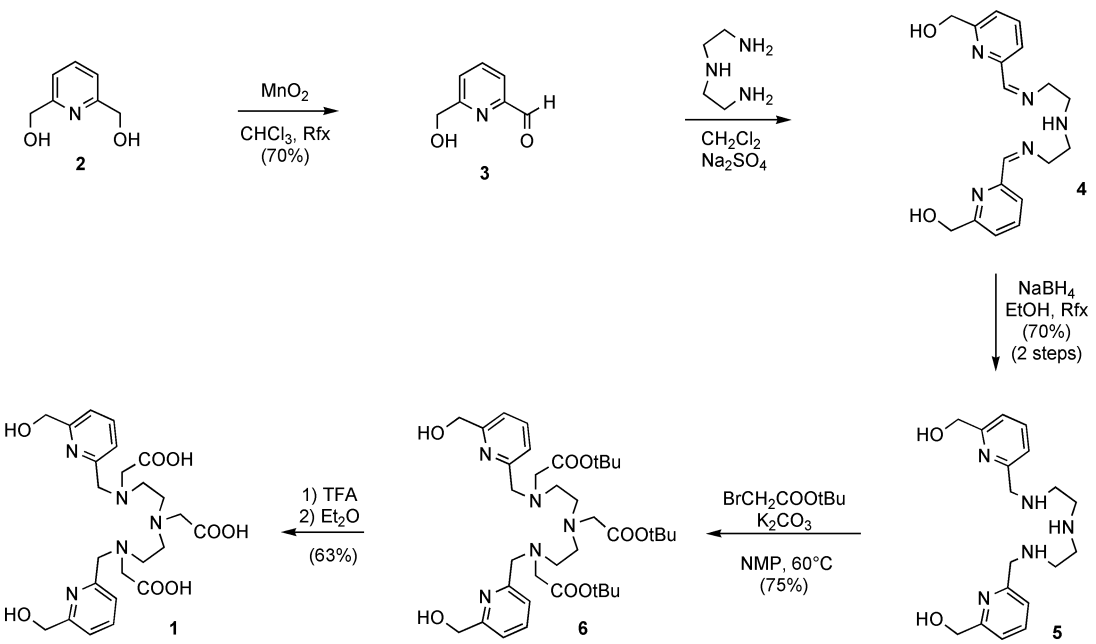

Scheme 1 Synthesis of ligand **1**.

Table 1 Resulting minimized geometries obtained using the Sparkle/AM1[12,13] semiempirical method

		Heat of formation/kcal mol^{-1}	Dipole moment/Debye	Ion potential/eV
Gd-1-H_2O	**1A**	−376.31	7.66	9.71
	1B	−377.30	8.68	9.55
	1C	−391.70	4.77	9.59

molecular orbital calculations use the Sparkle/AM1 method,[12,13] a computational chemistry model which is faster than *ab initio*/ECP calculations, with a comparable accuracy for ligands with directly coordinating nitrogen or oxygen atoms. The resulting (calculated) geometry of the coordination polyhedra for **Gd-1-H_2O** was in agreement with the ideal geometry of other Gd^{III} complexes with acyclic ligands, like Gd-DTPA,[14,15] Gd-BOPTA[16] and the neutral complex Gd-DTPA-BEA.[17] The arrangements of the donor atoms around the Gd^{III} metal ion, comprising two pyridine nitrogens, three amine nitrogens, three carboxylic oxygens and a water molecule, give rise to a nine-coordinated distorted tricapped trigonal prism (D_{3h} geometry, Fig. 2), according to Guggenberger and Muetterties,[18] who indicate that this kind of geometry is the preferred one for ML_9-type complexes.

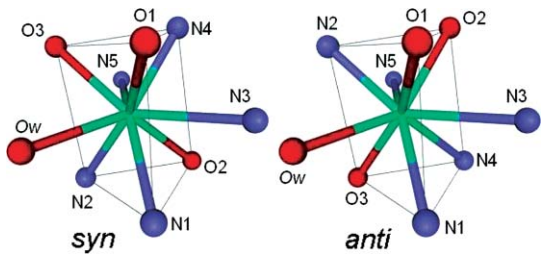

Fig. 2 Coordination polyhedron showing the tricapped trigonal prismatic coordination of the Gd^{III} atom, together with the two configurations arising from the mutual disposition of the two pyridine moieties.

This is confirmed also by the values of the dihedral angles between the mean least-square planes forming the faces of the coordination prism, values that compare favourably with those calculated for perfect D_{3h} geometry.[18]

For the **Gd-1-H_2O** complex, three minima geometries were found (structures **1A–C** in Table 1). The main difference between the three calculated structures is attributable to the mutual disposition of the two pyridine moieties (Fig. 2), a disposition that gives rise to a *syn* configuration for **1A** and **1B**, while **1C** adopts the *anti* configuration, which is the energetically favourable one, with an energy gap of ~14 kcal mol^{-1} (Table 1).

This difference led to a situation in the first two structures (**1A** and **1B**) where the capping positions are occupied by the oxygen atom of the coordinated water molecule (O_w) and by the terminal N2 and N4 nitrogen atoms of the polyaminopolycarboxylate ligand, while atoms N1, O2, N5 and O1, N3 and O3 constitute the vertices of the two triangular faces of the coordination polyhedron (*syn* configuration in Fig. 2). For **1C**, the capping positions are still occupied by O_w, N2 and N4, but in this case the vertices of the two triangular faces of the coordination polyhedron are now constituted by N1, N3, O3 and O1, O2 and N5, respectively (*anti* configuration in Fig. 2).

The Gd^{III} ion is near the centre of the prism for all of the structures, though shifted slightly towards the face capped by the water molecule (Table 2) and the triangular face, composed of the O1, N3, O3 donor atoms. This feature is common to other gadolinium complexes having a tricapped trigonal prism as the coordination polyhedron.

The mean Gd–N and Gd–$O_{carboxylate}$ distances compare well with those reported for other Gd^{III} complexes with acyclic ligands, while the Gd–O_{water} distance is slightly different with respect to those previously published. In particular, the analysis of the most stable structure (**1C**) shows for the Gd–O_{water} a bond length of 2.44 Å, very close to that found for other neutral complexes having a water molecule in the inner coordination sphere (2.42 Å for Gd-DTPA-BEA). The difference of 0.02 Å for this distance can be attributed to the presence (in **1C**) of two intermolecular hydrogen bonds (see Fig. 3) that can be responsible for both the lowest heat of formation and the shortening of the Gd–O_{water} distance.

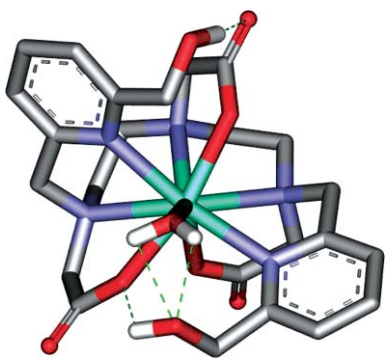

Fig. 3 View of the **1C** structure along the Ow-capped rectangular face, showing the intermolecular hydrogen bonds. Hydrogen atoms are not shown for clarity.

Relaxometric characterization of the Gd^{III} complex

The longitudinal proton relaxivities, r_{1p}, of Gd-**1**, GdDTPA and GdDTPA-BMA measured at 20 MHz, 25 °C and pH close to

Table 2 Distances (Å) involving the central nine-coordinated Gd^{III} atom

		O_w face	N2 face	N4 face	Gd–O_w	Gd–N1	Gd–N2	Gd–N3	Gd–N4	Gd–N5	Gd–O1	Gd–O2	Gd–O3
Gd-1-H_2O	**1A**	0.78	0.98	0.94	2.4111	2.5350	2.6295	2.6117	2.6411	2.5467	2.3880	2.3860	2.3999
	1B	0.78	1.03	0.97	2.4139	2.5649	2.6340	2.6592	2.6256	2.5759	2.4046	2.3877	2.3874
	1C	0.79	0.96	1.01	2.4355	2.5339	2.6421	2.6209	2.6090	2.5398	2.3946	2.3979	2.3941

neutrality are 4.03, 4.72 and 3.53 mM^{-1} s^{-1}, respectively. Thus, r_{1p} of Gd-**1** falls in the range of values typical of $q = 1$ systems and indicates that the complex has a 9-coordinate ground state with one inner sphere water molecule.[3] The occurrence of $q = 1$ also excludes the possible involvement of the OH groups of the ligand in the coordination of the metal ion. In addition, the intermediate relaxivity value between those for GdDTPA and GdDTPA-BMA suggests a mean residence lifetime, τ_M, of the bound water molecule sufficiently long so as to limit the relaxivity. In fact, it has been shown that the relevant difference in the relaxometric properties of GdDTPA and GdDTPA-BMA has to be attributed to their different τ_M values, *i.e.* $\tau_M = 300$ ns for the former and $\tau_M = 1.1$ μs for the latter (298 K).[19] Thus, all three complexes are likely to be isostructural, with an identical hydration state and with a small difference in relaxivity that can be accounted for in terms of different values of the exchange lifetime of the coordinated water molecule.

The pH dependence of the relaxivity, measured at 20 MHz and 298 K, confirms this hypothesis. In the case of Gd-**1** we observe a constant r_{1p} in the pH range 4 to 8 and an increase in both the acidic and basic regions (see ESI†). The increase from pH 4 to 1 is simply due to the progressive dissociation of the complex and release of the metal ion following the protonation of the basic sites of the ligand, as is typical for Gd^{III} complexes of acyclic polyaminopolycarboxylic ligands.[20] In the pH range 8 to 10, r_{1p} increases from 4.04 to 5.71 mM^{-1} s^{-1}. This behaviour parallels that observed in the case of cationic complexes and is interpreted in terms of the presence of an exceedingly long residence lifetime of the coordinated water molecule.[21] This allows the detection and evaluation of the effects associated with the prototropic exchange. In fact, at pH near neutrality, the proton exchange on a coordinated water molecule is much slower than the rate of exchange of the whole water molecule, but it can be significantly increased by catalysis of OH^- groups. When $\tau_M \geq$ *ca.* 1 μs, the prototropic exchange can make a dominant contribution to the overall (proton and oxygen) exchange rate at high pH values. Thus r_{1p} is limited by τ_M at neutral pH, but shows an increase due to the increase of k_{ex} at high pH values.[19,21]

A more reliable evaluation of the water exchange dynamics is provided by the measurement of the temperature dependence of the solvent water ^{17}O transverse relaxation rate, R_{2p}. In this experiment we extract information from the temperature dependence of the modulation of the Gd–Ow scalar interaction which depends directly on k_{ex} ($k_{ex} = 1/\tau_M$) and the electronic relaxation times $T_{1,2e}$.[22] Many low molecular weight Gd^{III} complexes have been investigated over the last 10 years and, as a consequence, a great deal of information has been acquired on the water exchange mechanisms and their dependence from the structural, electronic and stereochemical properties of the metal chelates.[22] The data are typically interpreted in terms of the Swift–Connick equations that depend on several parameters including: (i) the parameters related to the electronic relaxation times $T_{1,2e}$: *i.e.* the trace of the square of the zero-field splitting, Δ^2; the correlation time describing the modulation of the zero-field splitting, τ_V; and its activation energy, E_v; (ii) the enthalpy, $\Delta H_M^{\#}$, and entropy, $\Delta S_M^{\#}$, of activation for the water exchange process; (iii) the hyperfine Gd-$^{17}O_w$ coupling constant, $A/\hbar$.

The experimental data present maxima at low–intermediate temperatures for systems in relatively fast-exchange (*e.g.* GdDTPA) whereas they are shifted towards high temperatures for slowly-exchanging complexes (*e.g.* GdDTPA-BMA). In the case of Gd-**1** the experiment was carried out at 9.4 T and pH = 7 on a 16 mM solution of the complex over the range of temperatures 286 to 340 K. The results are plotted in Fig. 4 with the corresponding calculated curves for GdDTPA and GdDTPA-BMA. We clearly see that the R_{2p} values increase nearly exponentially by increasing temperature, in a manner quite similar to the behaviour observed for GdDTPA-BMA, to indicate a long value of τ_M. The parameters obtained from the fit of the data to the standard theory are reported in Table 3.

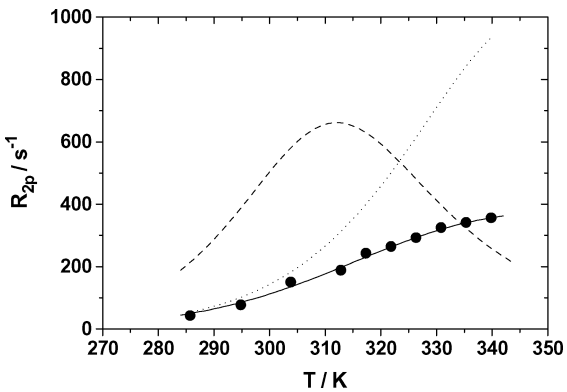

Fig. 4 Temperature dependence of the paramagnetic contribution to the water ^{17}O NMR transverse relaxation rate (R_{2p}) for Gd-**1**. Experimental conditions: 16.0 mM, pH 7.1, 9.4 T. The dashed and dotted lines represent curves for GdDTPA and GdDTPA-BMA, respectively.[23]

The water exchange lifetime at 298 K is *ca.* 2 μs, as for GdDTPA-BMA, and also very similar are their $\Delta H_M^{\#}$ and $A/\hbar$ values. The main difference of Gd-**1** over the other two complexes is the value of the electron relaxation parameters that most directly reflect the effects of the presence of a different set of donor groups in the new chelator.

NMRD. Having assessed the value of τ_M, we measured the magnetic field dependence of the proton relaxivity on a fast-field cycling relaxometer over the frequency range 0.01–70 MHz, at 298 K and pH = 7.1 (Fig. 5).

The relaxivity is constant from 0.01 to *ca.* 1 MHz, it shows a dispersion around 7 MHz and originates a small hump at

Table 3 Selected best-fit parameters obtained from the analysis of the $1/T_1$ NMRD profile (298 K, pH = 7.1) and ^{17}O NMR data (9.4 T) of Gd-**1**.

Parameter	Gd-**1**	Gd-DTPA-BMA[a]	Gd-DTPA[a]
Δ^2/s^{-2} 10^{-19}	12.1 ± 0.4	4.1 ± 0.2	3.6 ± 0.1
$^{298}\tau_V$/ps	7.0 ± 0.3	25 ± 1	25 ± 1
E_V/kJ mol^{-1}	2.5 ± 0.9	3.9 ± 1.4	1.6 ± 1.8
$^{298}\tau_M$/μs	2.4 ± 0.3	2.2 ± 0.1	0.30 ± 0.03
$\Delta H^{\#}_M$/kJ mol^{-1}	43.9 ± 0.6	47.6 ± 1.1	51.6 ± 1.4
$\Delta S^{\#}_M$/J mol^{-1} K^{-1}	+10.0 ± 1.7	+22.9 ± 3.6	+53 ± 4.7
$^{298}\tau_R$/ps	107 ± 5	66 ± 11	81 ± 2
r/Å[b]	3.10	3.15	3.1
q[b]	1	1	1
a/Å[b]	4.0	4.0	4.0
D/cm^2 s^{-1} 10^{-19}[b]	2.24	2.24	2.24

[a] From ref. 24. [b] Fixed during the least-squares procedure.

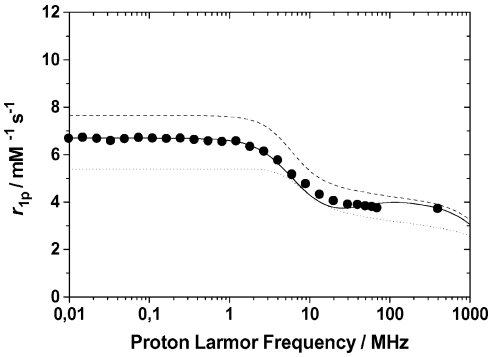

Fig. 5 $1/T_1$ NMRD profiles of Gd-**1** at pH = 7.1 and 298 K. The solid curve through the data points is calculated with the parameters reported in Table 1. The dashed and dotted lines represent the calculated NMRD profiles of GdDTPA and GdDTPA-BMA, respectively.[23]

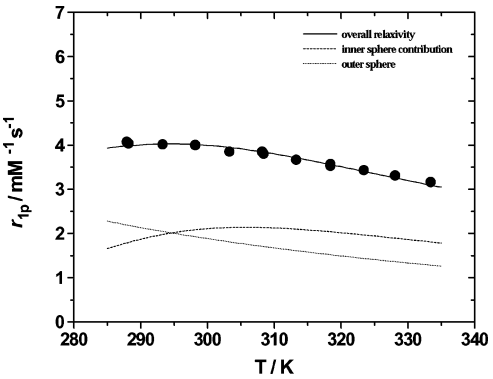

Fig. 6 Variable temperature proton relaxivity for Gd-**1**, at 20 MHz and pH = 7.1, showing the calculated inner and outer sphere contributions.

high fields. The calculated NMRD (nuclear magnetic relaxation dispersion) profiles for GdDTPA and GdDTPA-BMA are also reported for comparison. Clearly, the relaxivity is consistent with $q = 1$ and also evident is a quenching effect of the long τ_M at low fields, as for GdDTPA-BMA. The experimental data were fitted to the standard models of Solomon–Bloembergen–Morgan for the inner-sphere relaxation mechanism and Freed for the outer sphere components, by making reasonable assumptions for some of the physico-chemical parameters.[3] The diffusion coefficient, D, was set to 2.24×10^{-5} cm^2 s^{-1}, the distance of minimum approach of the outer sphere water molecules to the Gd^{III} was set to 4.0 Å, the hydration number q was fixed to 1, the distance between the metal ion and the protons of the bound water molecule was fixed to 3.1 Å and finally for τ_M we used the value obtained from the ^{17}O data. The result of the best fit procedure is very good and the experimental data are well reproduced with a value of 107 ps for the rotational correlation time τ_R and with values for Δ^2 and τ_V quite similar to those obtained from the analysis of the ^{17}O data. The τ_R value is significantly longer than for the other two complexes and reflects the larger size of Gd-**1** and it also explains the presence of a hump in the high magnetic fields region.

An alternative way of assessing the exchange dynamics of the coordinated water molecule is the measurement of the water proton relaxivity at a fixed frequency as a function of temperature. We performed the experiment at 20 MHz and analysed the data according to an established procedure, recently discussed in detail.[24] The data are shown in Fig. 6 along with the curves calculated with the parameters of Table 1. The outer sphere contribution to the relaxivity increases by decreasing temperature, whereas the inner sphere term has a maximum at *ca.* 310 K and, at lower temperatures, it decreases because of the limiting effect of the long τ_M value. The nice correspondence between the experimental and calculated data provides good support to the validity of the previous analysis.

Experimental

Reagents were obtained from Aldrich and used without further purification. ^{1}H-NMR and ^{13}C-NMR spectra were registered on a Jeol Eclipse ECP300 spectrometer at 300 MHz and 75.4 MHz, respectively. Mass spectra were performed on a ThermoFinningan LCQ-deca XP-PLUS, operating in ESI-MS mode. Elemental analyses were carried out with a Perkin Elmer Serie II CHNS/O 2400 analyzer.

6-Hydroxymethylpyridine-2-carboxaldehyde (2)

In a 500 mL round bottomed flask, 2,6-bis(hydroxymethyl)-pyridine (10.0 g, 71.9 mmol) is dissolved in hot trichloromethane (150 mL). The flask is cooled to room temperature and activated MnO_2 (12.5 g, 144 mmol) is slowly added. After the addition, the mixture is stirred and refluxed for 2 h, then further MnO_2 (10.0 g, 116 mmol) is added and reflux is resumed for a further 1 h.

The suspension is cooled and filtered through Celite®, washing the inorganic salts with methanol. The combined filtrate and washings are evaporated *in vacuo.* The oily residue is subjected to flash chromatography (silica gel, hexanes–ethyl acetate–2-propanol 85 : 5 : 10) obtaining pure **2**.

Yield 6.9 g (70%). Mp 63–65 °C (Lit.[25] 66–69 °C). Found: C, 61.08; H, 5.35; N, 10.17. Calc. for $C_7H_7NO_2$: C, 61.31; H, 5.14; N, 10.21%. Mass spectrum (ESI): m/z 138.2 (MH^+). Calc. for $C_7H_7NO_2$: 137.1 u.m.a.^{1}H-NMR ($CDCl_3$) 10.06 (s, 1H), 7.91–7.85 (m, 2H), 7.55–7.49 (m, 1H), 4.86 (s, 2H), 3.72 (bs, 1H). ^{13}C-NMR ($CDCl_3$) 193.2 [CH], 160.3 [C], 151.7 [C], 137.9 [CH], 125.0 [CH], 120.6 [CH], 64.2 [CH_2].

N,*N*″-Bis(6-hydroxymethyl-2-pyridylmethyl)diethylene-triamine (5)

In a 100 mL round bottomed flask, 6-hydroxymethylpyridine-2-carboxaldehyde (**2**, 6.62 g, 48.3 mmol) is dissolved in dichloromethane (20 mL). A solution of diethylenetriamine (2.49 g, 24.2 mmol) in dichloromethane (20 mL) is slowly added into the reaction flask, maintaining the temperature at <25 °C by means of a cold water bath. After the addition, sodium sulfate is added until the turbid emulsion becomes clear and homogeneous. The reaction mixture is stirred overnight and then filtered. The filtrate is evaporated *in vacuo* to give the crude diimine **4**. The latter is redissolved in methanol (50 mL). After cooling with an ice–water bath, sodium borohydride (1.83 g, 48.4 mmol) is added portionwise. The resulting solution is refluxed for 2 h, then cooled to room temperature. Conc. aqueous HCl is added dropwise until effervescence ceases, then the solution is brought to pH >10 with conc. aqueous ammonia and evaporated *in vacuo.* The solid residue is then purified by column chromatography

(silica gel, dichloromethane–methanol–conc. aq. NH_3 70 : 27 : 3), and dried *in vacuo* obtaining pure **5** as white powdery solid.

Yield 5.8 g (70%). Mp 76.2–78.8 °C. Found: C, 62.30; H, 8.01; N, 20.17. Calc. for $C_{18}H_{27}N_5O_2$: C, 62.59; H, 7.88; N, 20.27%. Mass spectrum (ESI): *m/z* 368.5 (MNa^+), 346.5 (MH^+). Calc. for $C_{18}H_{27}N_5O_2$: 345.4 u.m.a. ^{1}H-NMR (D_2O) 7.79 (t, 2H, $J = 8.0$ Hz), 7.42 (d, 2H, $J = 8.0$ Hz), 7.36 (d, 2H, $J = 8.0$ Hz), 4.63 (s, 4H), 4.11 (s, 4H), 3.08–2.96 (m, 8H). ^{13}C-NMR (D_2O) 159.6 [C], 152.4 [C], 139.2 [CH], 122.4 [CH], 121.3 [CH], 64.1 [CH_2], 51.6 [CH_2], 46.1 [CH_2], 45.1 [CH_2].

N,*N*″-Bis(6-hydroxymethyl-2-pyridylmethyl)-*N*,*N*′,*N*″-diethylenetriaminetriacetic acid tri-*tert*-butylester (6)

In a 10 mL round bottomed flask, compound **5** (0.600 g, 1.74 mmol) is dissolved in *N*-methylpyrrolidone (2 mL). Powdered potassium carbonate (1.082 g, 7.83 mmol) is added and the suspension stirred while *tert*-butyl bromoacetate (1.188 g, 6.09 mmol) is added dropwise in 10 min. The mixture is stirred at room temperature overnight, then filtered and the inorganic salts washed with dichloromethane. The combined filtrate and washings are evaporated *in vacuo*, and the oily residue subjected to column chromatography (silica gel, hexanes–ethyl acetate–2-propanol 80 : 15 : 5), obtaining pure **6** as slightly yellow oil.

Yield 0.897 g (75%). Found: C, 62.72; H, 8.44; N, 9.95. Calc. for $C_{36}H_{57}N_5O_8$: C, 62.86; H, 8.35; N, 10.18%. Mass spectrum (ESI): *m/z* 710.0 (MNa^+), 687.9 (MH^+). Calc. for $C_{36}H_{57}N_5O_8$: 687.0 u.m.a. ^{1}H-NMR ($CDCl_3$) 7.61 (t, 2H, $J = 7.6$ Hz), 7.36 (d, 2H, $J = 7.4$ Hz), 7.10 (d, 2H, $J = 7.7$ Hz), 4.70 (s, 4H), 3.90 (s, 4H), 3.33 (s, 2H), 3.29 (s, 4H), 2.77 (m, 8H), 1.44 (s, 18H), 1.40 (s, 9H). ^{13}C-NMR ($CDCl_3$) 170.8 [C], 170.7 [C], 158.7 [C], 158.4 [C], 137.2 [CH], 121.7 [CH], 118.9 [CH], 81.0 [C], 80.9 [C], 64.2 [CH_2], 60.1 [CH_2], 56.3 2 × [CH_2], 52.6 [CH_2], 52.4 [CH_2], 28.3 [CH_3], 28.2 [CH_3].

N,*N*″-Bis(6-hydroxymethyl-2-pyridylmethyl)-*N*,*N*′,*N*″-diethylenetriaminetriacetic acid (1)

In a 10 mL screw-cap vial, compound **6** (0.837 g, 1.22 mmol) is dissolved in neat trifluoroacetic acid (3.7 mL). The solution is stirred at room temperature overnight and then excess diethyl ether is added to precipitate the ligand, isolated by centrifugation and repeatedly washed with diethyl ether. The crude product is charged on a XAD-1600 column and eluted with a gradient water → water–methanol 100 : 0 → 50 : 50, collecting the fractions containing pure **1**. The combined fractions are evaporated *in vacuo* and the product dried under a high vacuum, obtaining compound **1** as a colourless glass.

Yield 0.399 g (63%). Found: C, 51.78; H, 6.92; N, 12.50. Calc. for $C_{24}H_{33}N_5O_8 \cdot 2H_2O$: C, 51.88; H, 6.71; N, 12.61%. Mass spectrum (ESI): *m/z* 542.2 (MNa^+), 520.2 (MH^+). Calc. for $C_{24}H_{33}N_5O_8$: 519.2 u.m.a. ^{1}H-NMR (D_2O) 7.79 (t, 2H, $J = 7.7$ Hz), 7.37 (m, 4H), 4.66 (s, 4H), 3.83 (s, 4H), 3.47 (s, 2H), 3.21 (s, 4H), 3.18 (t, 4H, $J = 5.8$ Hz), 2.92 (t, 4H, $J = 5.8$ Hz). ^{13}C-NMR (D_2O) 178.6 [C], 173.9 [C], 159.5 [C], 156.9 [C], 139.3 [CH], 123.5 [CH], 120.8 [CH], 64.4 [CH_2], 59.8 [CH_2], 57.9 [CH_2], 55.6 [CH_2], 51.5 [CH_2], 50.0 [CH_2].

^{1}H and ^{17}O relaxometry

The ^{1}H longitudinal water proton relaxation rates were measured at 20 MHz on a Spinmaster spectrometer (Stelar, Mede, Italy) operating in the range 0.45–1.6 T (corresponding to 20–70 MHz proton Larmor frequencies). The standard inversion recovery method was used with typical 90° pulse width of 3.5 μs, 16 experiments of 4 scans. The reproducibility of the T_1 data was ±4%. The temperature was controlled with a Stelar VTC-91 airflow heater equipped with a calibrated copper-constantan thermocouple (uncertainty of ±0.1 ° C). The proton $1/T_1$ NMRD profiles were measured on a Stelar fast field-cycling FFC-2000 (Mede, Pv, Italy) relaxometer on about 0.25–1.0 mmol gadolinium solutions in non-deuterated water. The relaxometer operates under computer control with an absolute uncertainty in $1/T_1$ of ±1%. The NMRD profiles were measured in the range of magnetic fields from 0.00024 to 1.6 T (corresponding to 0.01–70 MHz proton Larmor frequencies).

Variable-temperature ^{17}O NMR measurements were recorded on JEOL ECP-400 (9.4 T) spectrometer equipped with a 5 mm probe. Solutions containing 2.0% of the ^{17}O isotope (Cambridge Isotope) were used. The observed transverse relaxation rates were calculated from the signal width at half-height. Other details of the instrumentation, experimental methods, and data analysis have been previously reported.[24]

Conclusions

The pyridine group can be inserted into a diethylenetriamine backbone and act as a donor group towards lanthanide ions. The ligand **1** thus represents a new example of an octadentate ligand which forms neutral and stable complexes with trivalent lanthanide cations suitable for biomedical applications. A computational study suggests that the complex adopts a tricapped trigonal prismatic structural arrangement in which one capping position is occupied by a water molecule. The hydroxyl groups of the pyridine moieties form H-bonding interactions with the coordinated water molecule and, as a result, its mean residence lifetime is increased over that measured for GdDTPA and results in the complex being long enough to affect the water proton relaxation efficacy of the Gd^{III} derivative. This slow water exchange rate represents a clear limit for the development of Gd-based MRI CAs, but at the same time it could be of interest for the design of novel PARACEST agents.[26] Clearly, these hydroxyl groups could eventually be replaced by different, less hydrophilic moieties in order to weaken or remove the H-bonding interaction and enhance the rate of water exchange. Finally it must be outlined that in view of a possible *in vivo* utilization, a high kinetic and thermodynamic stability of the complex is required. This problem appears particularly critical for complexes with acyclic ligands and will be tackled in future work.

Acknowledgements

Financial support from CIRCMSB and PRIN 2005 is gratefully acknowledged.

Notes and references

1 (*a*) J.-C. Bünzli and G. R. Choppin, Lanthanide Probes in Life, Chemical and Earth Sciences, Elsevier, Amsterdam, 1989; (*b*) J. Rocha

and L. D. Carlos, *Curr. Opin. Solid State Mater. Sci.*, 2003, **7**, 199–205; (*c*) D. Parker, *Chem. Soc. Rev.*, 2004, **33**, 156–165; (*d*) J.-C. Bünzli and C. Piguet, *Chem. Soc. Rev.*, 2005, **34**, 1048–1077; (*e*) S. Pandya, J. Yu and D. Parker, *Dalton Trans.*, 2006, 2757–2766.
2 P. A. Rinck, Magnetic Resonance in Medicine, ABW Wissenschaftsverlag GmbH, Berlin, 2003.
3 (*a*) P. Caravan, J. J. Ellison, T. J. McMurry and R. B. Lauffer, *Chem. Rev.*, 1999, **99**, 2293–2352; (*b*) S. Aime, M. Botta and E. Terreno, Gd(III)-based Contrast Agents for MRI in *Advances in Inorganic Chemistry*, ed. R. van Eldik and I. Bertini, Elsevier, San Diego, 2005, vol. 57, pp. 173–237.
4 (*a*) L. Thunus and R. Lejeune, *Coord. Chem. Rev.*, 1999, **184**, 125–155; (*b*) F. Rosch and E. Forssell-Aronsson, *Met. Ions Biol. Syst.*, 2004, **42**, 77–108.
5 (*a*) M. A. Williams and H. Rapoport, *J. Org. Chem.*, 1994, **59**, 3616–3625; (*b*) I. Fraser Pickersgill and H. Rapoport, *J. Org. Chem.*, 2000, **65**, 4048–4057; (*c*) S. G. Gouin, J.-F. Gestin, A. Reliquet, J. C. Meslin and D. Deniaud, *Tetrahedron Lett.*, 2002, **43**, 3003–3005; (*d*) Y. Sun, A. E. Martell, J. H. Reibenspies, D. E. Reichert and M. J. Welch, *Inorg. Chem.*, 2000, **39**, 1480–1486; (*e*) H.-S. Chong, K. Garmestani, L. H. Bryant, Jr. and M. W. Brechbiel, *J. Org. Chem.*, 2001, **66**, 7745–7750.
6 (*a*) H. Schmitt-Willich, M. Brehm, C. L. J. Ewers, G. Michl, A. Müller-Fahrnow, O. Petrov, J. Platzek, B. Radüchel and D. Sülzle, *Inorg. Chem.*, 1999, **38**, 1134–1144; (*b*) P. Caravan, N. J. Cloutier, M. T. Greenfield, S. A. McDermid, S. U. Dunham, J. W. M. Bulte, J. C. Amedio, Jr., R. J. Looby, R. M. Supkowski, W. D. Horrocks, Jr., T. J. McMurry and R. B. Lauffer, *J. Am. Chem. Soc.*, 2002, **124**, 3152–3162; (*c*) S. Laurent, F. Botteman, L. Vander Elst and R. N. Muller, *Helv. Chim. Acta*, 2004, **87**, 1077–1089; (*d*) D. Imbert, N. Fatin-Rouge and J.-C. Bünzli, *Eur. J. Inorg. Chem.*, 2003, 1332–1339.
7 (*a*) P. Caravan, P. Mehrkhodavandi and C. Orvig, *Inorg. Chem.*, 1997, **36**, 1316–1321; (*b*) R. Dickins, D. Parker, J. I. Bruce and D. J. Tozer, *Dalton Trans.*, 2003, 1264–1271.
8 R. Ziessel, P. Nguyen, L. Douce, M. Cesario and C. Estournes, *Org. Lett.*, 2004, **6**, 2865–2868.
9 (*a*) A. F. Abdel-Magid, K. G. Carson, B. D. Harris, C. A. Maryanoff and R. D. Shah, *J. Org. Chem.*, 1996, **61**, 3849–3862; (*b*) A. F. Abdel-Magid and S. J. Mehrmann, *Org. Process Res. Dev.*, 2006, **10**, 971–1031.
10 G. B. Giovenzana, G. Jommi, R. Pagliarin, M. Sisti, S. Aime, M. Botta and S. Geninatti Crich, *Recl. Trav. Chim. Pays-Bas*, 1996, **115**, 94–98.
11 T. R. Cundari, E. W. Moody and S. O. Sommerer, *Inorg. Chem.*, 1995, **34**, 5989–5999.
12 G. B. Rocha, R. O. Freire, N. B. da Costa, Jr, G. F. de Sá and A. M. Simas, *Inorg. Chem.*, 2004, **43**, 2346–2354.
13 R. O. Freire, G. B. Rocha and A. M. Simas, *Inorg. Chem.*, 2005, **44(9)**, 3299–3310.
14 H. Gries and H. Miklautz, *Physiol. Chem. Phys. Med. NMR*, 1984, **16**, 105–112.
15 M. B. Inoue, M. Inoue and Q. Fernando, *Inorg. Chim. Acta*, 1995, **232**, 203–210.
16 F. Uggeri, S. Aime, P. L. Anelli, M. Botta, M. Brocchetta, C. de Haen, G. Ermondi, M. Grandi and P. Paoli, *Inorg. Chem.*, 1995, **34**, 633–642.
17 M. S. Konings, W. C. Dow, D. B. Love, K. N. Raymond, S. C. Quay and S. M. Rocklage, *Inorg. Chem.*, 1990, **29**, 1488–1491.
18 L. J. Guggenberger and E. L. Muetterties, *J. Am. Chem. Soc.*, 1976, **98**, 7221–7225.
19 S. Aime, M. Botta, M. Fasano and E. Terreno, *Acc. Chem. Res.*, 1999, **32**, 941–949.
20 A. E. Merbach and E. Tóth, The Chemistry of Contrast Agents in Medical Magnetic Resonance Imaging, John Wiley & Sons, Chichester, 2001.
21 S. Aime, A. Barge, J. I. Bruce, M. Botta, J. A. K. Howard, J. M. Moloney, D. Parker, A. S. de Sousa and M. Woods, *J. Am. Chem. Soc.*, 1999, **121**, 5762–5771.
22 L. Helm, E. Tóth and A. E. Merbach, in Metal Ions in Biological Systems, ed. A. Sigel and H. Sigel, Marcel Dekker Inc., New York, 2003, ch. 15.
23 D. H. Powell, O. M. Ni Dhubhghaill, D. Pubanz, L. Helm, Y. S. Lebedev, W. Schlaepfer and A. E. Merbach, *J. Am. Chem. Soc.*, 1996, **118**, 9333–9346.
24 L. Thompson, D. Parker, D. A. Fulton, J. A. K. Howard, S. U. Pandya, H. Puschmann, K. Senanayake, P. A. Stenson, A. Badari, M. Botta, S. Avedano and S. Aime, *Dalton Trans.*, 2006, 5605–5616.
25 Y. Okuyama, K. Nakano, E. Nozawa, K. Takahashi and H. Hongo, *Heterocycles*, 2002, **58**, 457–460.
26 M. Woods, D. E. Woessner and A. D. Sherry, *Chem. Soc. Rev.*, 2006, **35**, 500–511.